COBEM 2021 Florianópolis - Brasil
26th ABCM International Congress of Mechanical Engineering
November 22-26, 2021. Florianópolis, SC, Brazil

COB-2021-0524
MULTIVARIABLE CONTROL ANALYSIS OF AN ACTIVE SUSPENSION SYSTEM

Felipe Marques Farias Filho
Lucas da Silva Rigobello
Maíra Martins da Silva
Marcelo Becker
University of São Paulo, São Carlos School of Engineering, Avenida Trabalhador São-carlense, 400, CEP 13566-590 - São Carlos - SP- Brasil
fmfariasfilho@usp.br, lucasrigobell@usp.br, mairams@sc.usp.br, becker@sc.usp.br

Abstract. *Comfort is one of the most valued features of passenger cars. It can be improved by developing active suspension systems targeting to control the wheels' vertical movements and the vehicle, correcting and compensating for imperfections in the track with greater efficiency than the standard suspension system. One alternative to control these dynamic systems is to use optimal control, like Linear Quadratic Regulators (LQR), which are full-state feedback controllers whose tuning depends on weight coefficient matrices. Usually, these coefficients are determined by experience and trial. For large systems, this might be an arduous task. In addition, a disadvantage of this type of controller is its lack of robustness. This work aims to design an LQR controller for an active suspension system modeled with four degrees of freedom. In this proposal, the weight coefficients are derived by solving an optimization problem that considers different sources of uncertainty in the model: vehicle mass, tire stiffness, and damping coefficients of the front and rear suspension. The optimization problem created for obtaining the weight coefficients was solved using the Pattern Search algorithm. The objective function considers the vehicle's vertical acceleration, required actuation energy, and a contact index between the vehicle and the track. Three alternatives for the controller are analyzed considering different weights for the energy-related term. These are compared with the standard system when excited by a bump. The same terms of the objective function have been used for this comparison. The designed systems reduced the settling times and amplitudes of the vehicle's vertical acceleration. The characteristics of the track contact index have been little affected. Therefore, the designed active suspension system is able to provide more comfort and still maintain the vehicle's controllability, hence preserving its safety features.*

Keywords: *Active suspension, LQR, Control, Optimization, Pattern Search*

1. INTRODUCTION

Regarding passenger cars, comfort comes as one of the most valued features by drivers and passengers. In this aspect, the suspension system plays a key role in transmitting the forces and disturbances from the ground to the car body and consequently into the vehicle. The passive suspension is the most common suspension system found in passenger cars, but semi-active and active suspensions are also found. This active type provides control in the variation of spring stiffness and damping. In terms, it can control the vertical movements of the wheels and the vehicle, correcting and compensating for road imperfections more efficiently. In this way, the active suspension stands out for having the best characteristics to deal with the different conditions imposed by the roads (SUN *et al.*, 2020). It ensures greater comfort, besides providing stability gain to the vehicle, such as in situations of curves, acceleration, or braking, consequently resulting in better drivability for the driver (dos Santos, 2010).

Concerning the development process of an active suspension, some vehicle model configurations can be found in the literature. Figure 1 brings the three most common model configurations: 2 degrees-of-freedom (DOF), composed of two masses, a quarter of the vehicle mass and the mass of a wheel; 4 DOF, half of the vehicle mass, and two wheels; and 7 DOF, which considers the four wheels of the vehicle and its total mass.

To investigate the improvement in ride comfort using the active suspension, the control strategy is simulated with the chosen model. A quarter car model was used by Kumar and Vijayarangan (2006), integrating with a Linear Quadratic Regulator (LQR), assuming two different approaches, the conventional method and another dependent on acceleration; then compared with a passive suspension. As result, the tires and road contact force, and ride comfort are improved with the active suspension. The half-car model was used by Pang *et al.* (2017), which presented an improved linear quadratic and Gaussian distributed (LQG) controller, that evaluated the coefficients through a genetic algorithm, considering no

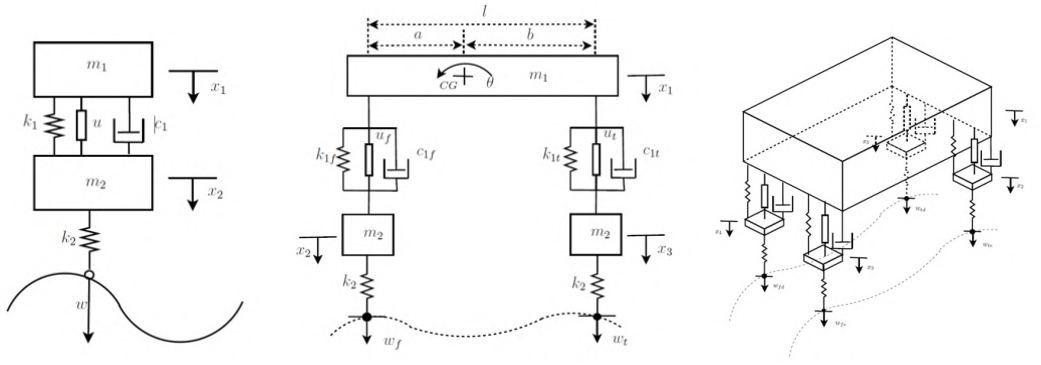

(a) (b) (c)

Figure 1: Simplified vehicle models, a) quarter car, b) half car, and c) full car (dos Santos, 2010)

road input signals, since these are unknown conditions. Full car model active suspension was conducted by Darus and Sam (2009) and successful results were also found using LQR, simulating two types of road profiles for input disturbance.

Hasbullah and Faris (2010), based on a half car model, presented that the LQR and Fuzzy Logic Controller (FLC) had a better performance than the passive system, since having the worst settling time, even showing the smallest percentage overshoot. The LQR performance stood out with a small percentage overshoot and faster settling time. While fuzzy logic controller needs less force to control the actuator. Another investigation, under random road profile (ISO 8608), showed that settling time and amplitude of the road disturbances were improved with the Adaptive Neuro Fuzzy Inference System (ANFIS), compared to LQR, Proportional Integral Derivative (PID), and the passive system (Gandhi *et al.*, 2017). Another investigation with a quarter model car and LQR, against the H ∞, is driven in the time domain, asserting better performance of LQR controller to improve vehicle ride comfort (Nagarkar and Patil, 2012).

In this context, this work aims to obtain an LQR controller that provides a more comfortable and safer suspension for passengers. Making use of the 4 DOF model, it becomes feasible to analyze the vertical motion of each wheel and the vehicle, as well as the vehicle's angular motion, called pitch. In addition, in the considered model, the exogenous inputs will be the displacements coming from disturbances, from track irregularities. That is, they are the excitations coming from the track on the front and rear suspensions, respectively indicated by w_f and w_t. The manipulated inputs, on the other hand, are the forces applied by the active suspension actuators installed on the front and rear suspensions, u_f and u_t, respectively.

The comfort is determined using the value of the vertical acceleration of the car; and safety is related to a defined index, representing the contact between the tire and the ground. Defining two main parameters that must be handled side by side. Therefore, the controlled outputs are the vehicle vertical acceleration, vehicle angular acceleration, asphalt contact index, and the control efforts of both the front and rear suspension. The controlled outputs will be discussed in more detail, gathering their respective mathematical formulations, in the performance formulation section.

As discussed by Doyle (1978), the LQR controller does not have a guaranteed robustness range. Thus, to ensure the performance of the controller, four sources of uncertainty were taken into account for the model: the vehicle mass, tire stiffness, and each suspension damper. The vehicle mass variation was considered because the vehicle may or may not be at its maximum passenger and cargo capacity. The tire stiffness variation was taken into account, since the tire may not be properly calibrated. Finally, the variation of the suspension shock absorber was considered, since its functioning can be affected by wear and temperature variation. In all uncertainty sources, the adopted variation was from -15% to $+15\%$ of the nominal value.

2. MODEL DEVELOPMENT

As described earlier, a four DOF model is employed in this work and it is depicted in Fig. 1(b), which represents the vertical motion of the vehicle, the wheels, and the pitch motion. This dynamic model takes into account the stiffness and damping of the front and rear suspension, represented by the parameters k_{1f}, k_{1t}, c_{1f}, c_{1t}. Other parameters are the stiffness of the tires (k_2), half the mass of the vehicle (m_1), and the mass of each of the tires (m_2). The values assumed for each of these parameters are shown in Table 1. Table 2 presents the equivalent values for the extreme cases taking into account the uncertainties of the vehicle mass, spring stiffness, and suspension damping parameters.

In representation of space state, the model defined by the Eq. 1, which the equations deduction were based on Santos (2010), presents the following state parameters $\{\boldsymbol{x}\}^T = (x_1, x_2, x_3, x_4, x_5, x_6, x_7, x_8)^T$, and $\{\dot{\boldsymbol{x}}\} = d\boldsymbol{x}/dt$. Where x_1 is the vertical displacement of the vehicle, x_2 is the vertical displacement of the front wheel, x_3 is the vertical displacement of the rear wheel, x_4 the angular pitch displacement (θ), x_5 the vertical speed of the vehicle, x_6 the vertical speed of the front wheel, x_7 the vertical speed of the rear wheel, and x_8 the angular speed of the vehicle ($\dot{\theta}$). On the other hand, u_f and

Table 1: Nominal parameter values for the 4 DOF model

Parameter	Value
m_1	$750\ kg$
m_2	$59\ kg$
Moment of inertia (I)	$2160\ kg\ m^2$
c_{1f}	$1000\ Ns/m$
c_{1f}	$1100\ Ns/m$
k_{1f}	$35000\ N/m$
k_{1t}	$38000\ N/m$
k_2	$190000\ N/m$
Vehicle Length (l)	$3.1\ m$
Distance to front (a)	$1.4\ m$
Distance to rear (b)	$1.7\ m$

(dos Santos, 2010)

Table 2: Parameter values for the 4 DOF model

	Parameters with uncertainty			
	$m_1[kg]$	$c_{1f}[Ns/m]$	$c_{1t}[Ns/m]$	$k_2[N/m]$
Case 1	862.5	1150.0	1265.0	218500.0
Case 2	637.5	1150.0	1265.0	218500.0
Case 3	862.5	850.0	935.0	218500.0
Case 4	637.5	850.0	935.0	218500.0
Case 5	862.5	1150.0	1265.0	161500.0
Case 6	637.5	1150.0	1265.0	161500.0
Case 7	862.5	850.0	935.0	161500.0
Case 8	637.5	850.0	935.0	161500.0

(dos Santos, 2010)

u_t are the control forces exerted by the actuators on each of the wheels, and w_f and w_t are the displacements imposed on each of the wheels due to the track disturbances, representing the system inputs. The matrices $[\mathbf{A}]$, $[\mathbf{B_1}]$ and $[\mathbf{B_2}]$ are presented below by Eqs. 2 and 3.

$$\begin{aligned}\{\dot{\boldsymbol{x}}\} &= [\mathbf{A}]\{\boldsymbol{x}\} + [\mathbf{B_1}]\{\boldsymbol{u}\} + [\mathbf{B_2}]\{\boldsymbol{w}\} \\ \{\boldsymbol{z}\} &= [\mathbf{C}]\{\boldsymbol{x}\} + [\mathbf{D_1}]\{\boldsymbol{u}\} + [\mathbf{D_2}]\{\boldsymbol{w}\}\end{aligned} \tag{1}$$

$$\mathbf{A} = \begin{bmatrix} 0 & 0 & 0 & 0 & 1 & 0 & 0 & 0 \\ 0 & 0 & 0 & 0 & 0 & 1 & 0 & 0 \\ 0 & 0 & 0 & 0 & 0 & 0 & 1 & 0 \\ 0 & 0 & 0 & 0 & 0 & 0 & 0 & 1 \\ \frac{-k_{1f}-k_{1t}}{m_1} & \frac{k_{1f}}{m_1} & \frac{k_{1t}}{m_1} & \frac{k_{1f}b-k_{1t}a}{m_1} & \frac{-c_{1f}-c_{1t}}{m_1} & \frac{c_{1f}}{m_1} & \frac{c_{1t}}{m_1} & \frac{c_{1f}b-c_{1t}a}{m_1} \\ \frac{k_{1f}}{m_2} & \frac{-k_{1f}-k_2}{m_2} & 0 & \frac{k_{1f}a}{m_2} & \frac{c_{1f}}{m_2} & \frac{-c_{1f}}{m_2} & 0 & \frac{c_{1f}a}{m_2} \\ \frac{k_{1t}}{m_2} & 0 & \frac{-k_{1t}-k_2}{m_2} & \frac{k_{1t}b}{m_2} & \frac{c_{1t}}{m_2} & 0 & \frac{-c_{1t}}{m_2} & \frac{c_{1t}b}{m_2} \\ \frac{k_{1f}b-k_{1t}a}{I} & \frac{k_{1f}a}{I} & \frac{-k_{1t}b}{I} & \frac{-k_{1f}b^2-k_{1t}a^2}{I} & \frac{c_{1f}b-c_{1t}a}{I} & \frac{c_{1f}a}{I} & \frac{-c_{1t}b}{I} & \frac{-c_{1f}b^2-c_{1t}a^2}{I} \end{bmatrix} \tag{2}$$

$$\mathbf{B_1} = \begin{bmatrix} 0 & 0 \\ 0 & 0 \\ 0 & 0 \\ 0 & 0 \\ 1/m_1 & 1/m_1 \\ -1/m_2 & 0 \\ 0 & -1/m_2 \\ -a/I & b/I \end{bmatrix} \quad \mathbf{B_2} = \begin{bmatrix} 0 & 0 \\ 0 & 0 \\ 0 & 0 \\ 0 & 0 \\ 0 & 0 \\ k_2/m_2 & 0 \\ 0 & k_2/m_2 \\ 0 & 0 \end{bmatrix} \tag{3}$$

2.1 Performance Functions

This work takes into consideration four aspects that characterize the suspension performance, the same way it was presented by dos Santos (2010). These aspects are passenger comfort, safety, and the control effort in the front and rear actuator. For comfort, it is intended to design the controller to work in the frequency range of 4 to 8 Hz, because it corresponds to a range of excitation more sensitive to humans, as cited in ISO-2631-1 (2010), thus being employed the performance measure given by z_1 as presented by:

$$\begin{aligned}z_1 = \ddot{x}_1 = \dot{x}_5 = -\tfrac{k_{1f}+k_{1t}}{m_1}x_1 + \tfrac{k_{1f}}{m_1}x_2 + \tfrac{k_{1t}}{m_1}x_3 + \tfrac{k_{1t}b-k_{1f}a}{m_1}x_3 - \tfrac{c_{1f}+c_{1t}}{m_1}x_5 + \tfrac{c_{1f}}{m_1}x_6 + \tfrac{c_{1t}}{m_1}x_7 + \dots \\ \cdots + \tfrac{c_{1t}b-c_{1f}a}{m_1}x_8 + \tfrac{u_f}{m_1} + \tfrac{u_t}{m_1}\end{aligned} \tag{4}$$

Another performance aspect contributing to comfort is angular acceleration, shown by z_2, as given by Eq. 5. And similar to the previous case, according to the ISO-2631-1 (2010) standard, for angular accelerations, humans are most sensitive to the frequency range of 1 to 2 Hz.

$$z_2 = \ddot{\theta} = \dot{x}_8 = \frac{k_{1f}b - k_{1t}a}{I}x_1 + \frac{k_{1f}a}{I}x_2 - \frac{k_{1t}b}{I}x_3 - \frac{k_{1f}b^2 + k_{1t}a^2}{I}x_4 + \frac{c_{1f}b - c_{1t}a}{I}x_5 + \frac{c_{1f}a}{I}x_6 - \dots \\ \dots - \frac{c_{1t}b}{I}x_7 - \frac{c_{1f}b^2 + c_{1t}a^2}{I}x_8 - \frac{au_f}{I} + \frac{bu_t}{I} \tag{5}$$

Already, in terms of safety, it is desired that the wheels don't lose contact with the ground. In that way, the performance measure is defined by z_3, named as the relative displacement of the wheels, given by Equation 6, obtained as a maximization of the contact with the track, by calculating the momentum imposed on the vehicle and making $M_{ext} = 0$.

$$z_3 = b(x_3 - w_t) - a(x_2 - w_f) \tag{6}$$

And finally, because it is an active suspension, it is necessary to use actuators. In this regard, two other performance measures z_4 and z_5 have been defined as a function of the actuators control effort, given by Equations 7 and 8.

$$z_4 = \left| u_f(\dot{x}_1 + a\dot{\theta}) \right| + |u_f \dot{x}_2| \tag{7}$$

$$z_5 = \left| u_t(\dot{x}_1 + b\dot{\theta}) \right| + |u_t \dot{x}_3| \tag{8}$$

2.2 Plant Analysis

The controllability matrix is calculated for each one of the extreme cases, given by $\mathbb{C} = [\mathbf{B}\ \mathbf{AB}\ \dots\ \mathbf{A}^{n-1}\mathbf{B}]$. If the rank of the controllability matrix is equal to the rank of $[\mathbf{A}]$, it implies that the system is completely controllable (Ogata, 2010). The condition for complete controllability is necessary, and sufficient, to guarantee that a state feedback controller can be used (Ogata, 2010). After this analysis, it was verified that all extreme cases are completely controllable, *i.e.*, the LQR controller, which is a state feedback controller can be applied.

3. LQR CONTROLLER

Given that the proposed model, the half-vehicle model, can be represented in state-space as presented in the relation provided by Eq. 1. To design an LQR type controller, one must assume, since it is a state feedback controller, that the measurement of all states is available, or they can be estimated.

Thus, the LQR control system can be described as follows. Starting with the state feedback control law $\boldsymbol{u} = -\mathbf{K}\boldsymbol{x}$, where $\mathbf{K}$ is the feedback gain matrix (Ogata, 2010). The optimization method consists of the determination of the control input $\boldsymbol{u}$ that minimizes the performance cost defined by J, which considers the performance requirements and the input limitations of the controller, expressed by Eq. 9.

$$J = \int_0^\infty (\boldsymbol{x}^T\mathbf{Q}\boldsymbol{x} + \boldsymbol{u}^T\mathbf{R}\boldsymbol{u} + 2\boldsymbol{x}^T\mathbf{N}\boldsymbol{u})\, dt \tag{9}$$

where $\mathbf{Q}$, $\mathbf{R}$ and $\mathbf{N}$ are positive defined weight matrices. For the controller determination, the system must be completely controllable. Furthermore, the algebraic Riccati equation, Eq. 10, must be satisfied, from which it is obtained the matrix $\mathbf{P}$, necessary to define the optimal gain matrix $\mathbf{K}$, obtained by Eq. 11.

$$\mathbf{AP} + \mathbf{A}^T\mathbf{P} - \mathbf{PBR}^{-1}\mathbf{B}^T + \mathbf{Q} = 0 \tag{10}$$

$$\mathbf{K} = \mathbf{R}^{-1}\mathbf{B}^T\mathbf{P} \tag{11}$$

Thus, the optimized closed-loop system is obtained by Eq. 12.

$$\dot{\boldsymbol{x}} = ([\mathbf{A}] - [\mathbf{B_1K}])\{\boldsymbol{x}\} + [\mathbf{B_2}]\{\boldsymbol{w}\} \tag{12}$$

4. SIMULATION AND OPTIMIZATION

4.1 Simulation

For the simulation, it was proposed the use of a speed bump disturbance with ellipsoid profile, height 0.1 m, and length 0.5 m, provided by Eq. 13. Also, for the simulation, the vehicle velocity adopted was 40 km/h, which results in a delay between the input in the front wheels and the rear wheels of 0.324 s. Figure 2 represents the disturbance profile forced by the speed bump and the delay between the front wheels and the rear wheels.

$$y = 0.1\sqrt{1 - \frac{x^2}{0.25^2}} \tag{13}$$

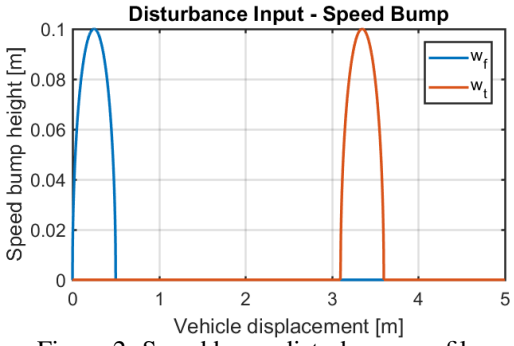

Figure 2: Speed bump disturbance profile

4.2 Optimization

Considering that the selection of the LQR weight coefficients depends on expert experience and testing, Pang *et al.* (2017) proposed the application of Genetic Algorithm (GA) optimization as a way to reduce the design time and avoid subjectivity. Following the same premise, this work proposes using optimization techniques to determine the weights of the LQR controller matrices. The optimization routine chosen was the Pattern Search.

The Pattern Search algorithm, also known as Powell's Method, is classified within the category of unconstrained optimization methods, more specifically, as a direct search method for not calculating the objective function's gradient (Rao, 2019). Pattern Search is an evolution of the univariate method. The search for the optimal result is done in orthonormal directions. Only one design variable is allowed to change, while the other ones are constant. In the Pattern Search method, this search is done in conjugated directions, which are combinations of the orthonormal directions.

This method was chosen due to the absence of the objective function's gradient. Even though it is an unconstrained method, restrictions can be easily added, as seen ahead. A disadvantage of this strategy is that it needs an admissible point. In this work, this was not a problem because any positive set of the design variables, within the imposed bounds, results in an admissible point.

The design variables used in this work's optimization problem were the weight coefficients of the matrices $\mathbf{Q}$ and $\mathbf{R}$ of the LQR controller, as illustrated in Eq. 14.

$$\mathbf{Q} = \begin{bmatrix} x_1 & 0 & \dots & 0 \\ 0 & x_2 & & \vdots \\ \vdots & & \ddots & \\ 0 & \dots & & x_8 \end{bmatrix} \; and \; \mathbf{R} = \begin{bmatrix} x_9 & 0 \\ 0 & x_{10} \end{bmatrix} \tag{14}$$

The objective function created in this work is presented in Eq. 15.

$$f(x_1, x_2, \dots, x_{10}) = \left\|G_{MF_{z_1}}\right\|_\infty + C_1 \left\|G_{MF_{z_3}}\right\|_\infty + C_2(\left\|G_{MF_{potf}}\right\|_\infty + \left\|G_{MF_{pott}}\right\|_\infty) \tag{15}$$

where $\left\|G_{MF_{z_1}}\right\|_\infty$ is the H_∞ norm of the vertical acceleration closed-loop transfer function due to the disturbance in the front suspension, $\left\|G_{MF_{z_3}}\right\|_\infty$ is the H_∞ norm of the contact index closed-loop transfer function due to disturbance in the front suspension, $\left\|G_{MF_{potf}}\right\|_\infty$ and $\left\|G_{MF_{pott}}\right\|_\infty$ are the H_∞ norm of the front and rear suspension power transfer

functions, respectively. The constants C_1 and C_2 are weights added to manually modify to achieve better results. Three projects were created varying these constants. Table 3 presents the values used in each one of these projects. The search space was bounded by the lower bound 0, and upper bound of 10^{12}. The lower bound was used to avoid the matrices $\mathbf{Q}$ and $\mathbf{R}$ becoming singular, and the upper bound was used to avoid the system to become unstable. The initial point adopted in all projects was $x = [1, 1, 1, 1, 1, 1, 1, 1, 1, 1]$. Equation 16 shows the explicit optimization problem.

$$\begin{aligned} \min_{x_1,x_2,\ldots,x_{10}} \quad & f(x_1, x_2, \ldots, x_{10}) = \left\|G_{MF_{z_1}}\right\|_\infty + C_1 \left\|G_{MF_{z_3}}\right\|_\infty + C_2(\left\|G_{MF_{potf}}\right\|_\infty + \left\|G_{MF_{pott}}\right\|_\infty) \\ \text{s.t.} \quad & 0 < x_1, x_2, \ldots, x_{10} \leq 10^{12} \end{aligned} \tag{16}$$

Table 3: Constants C_1 and C_2

Project	C_1	C_2
1	4	0
2	3	1/30
3	3	1/40

5. RESULTS AND DISCUSSION

5.1 Optimized Controller

As explained, this work investigates three LQR controller designs, which were obtained by applying an optimization method to determine the elements of the weight matrices $\mathbf{Q}$ and $\mathbf{R}$. As a result of the optimization, Table 4 presents the optimal values of the design variables, resulting in their respective controller designs as presented in Table 5.

Table 4: Optimal weight coefficients of each design

	x_1	x_2	x_3	x_4	x_5	x_6	x_7	x_8	x_9	x_{10}
Project 1	39161	1	1029	2E+06	1.00E+12	1	1	1	1	1
Project 2	1626	257	4	4E+05	1.67E+09	1	1	1	1	1
Project 3	2240	257	4	4E+05	2.95E+09	1	1	1	1	1

Table 5: Resulting $\mathbf{K}$ matrices for each design

	Resulting K matrix							
Project 1	-1025.2	571.9	584.5	1659.0	672649.7	16.5	17.0	50.2
	-1128.9	595.8	680.0	-1010.5	739894.0	17.0	19.7	-30.6
Project 2	4248.4	-13079.0	-14086.0	5975.2	28036.0	277.7	304.6	-152.4
	-7535.9	-14101.0	-14253.0	7553.7	27734.0	267.3	282.8	541.5
Project 3	4289.9	-14072.0	-14920.0	6138.8	37635.0	324.2	356.4	-145.3
	-7646.9	-15273.0	-15266.0	7717.0	37223.0	309.8	330.2	549.8

5.2 Frequency response analysis

Therefore, the three controllers designed have different response characteristics. An analysis is performed comparing the frequency response of the system controlled with each of these controllers. Figure 3 shows the frequency response of the system with and without control, for vertical acceleration. Figure 4 presents the frequency response for angular acceleration. In both cases, it can be observed that there was a reduction of the response amplitude in the desired frequency ranges. Except for the first design, where the angular acceleration showed little variation. Figure 5 gives the frequency response of the system with and without control, for the relative displacement performance parameter that relates the tire contact with the ground. In this case, there was a significant gain at low frequencies, but there was a reduction in the gain corresponding to one of the peaks of the system's vibration modes.

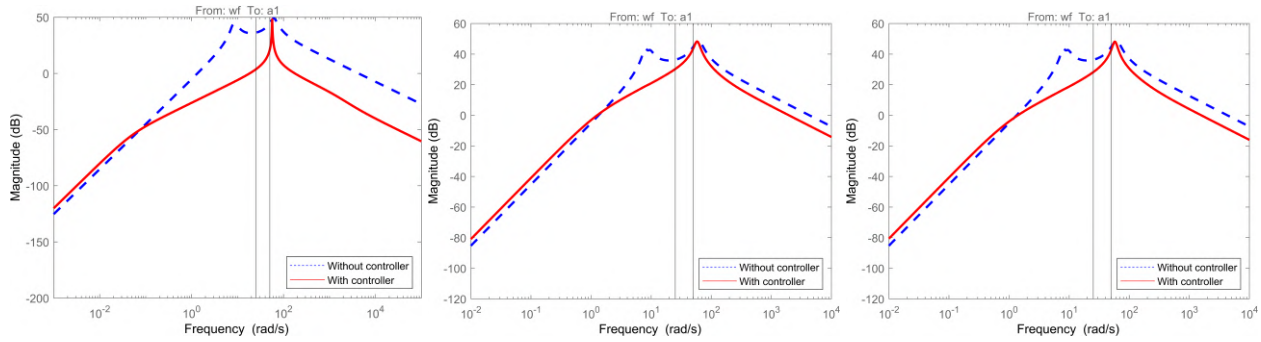

(a) (b) (c) t!

Figure 3: Frequency response of vertical acceleration: a) design 1; b) design 2; c) design 3. The vertical lines delimit the range of greatest sensitivity for humans according to ISO 2631-1

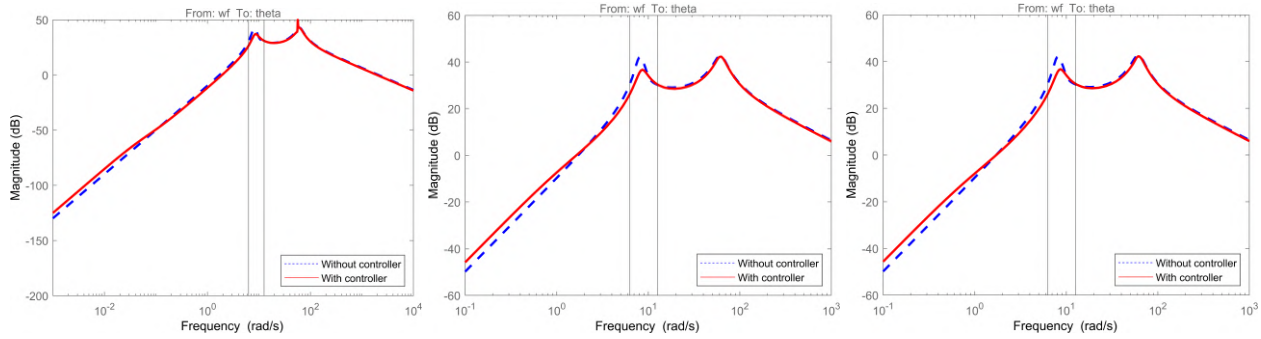

(a) (b) (c)

Figure 4: Frequency response of angular acceleration: a) design 1; b) design 2; c) design 3. The vertical lines delimit the most sensitive range for humans according to ISO 2631-1

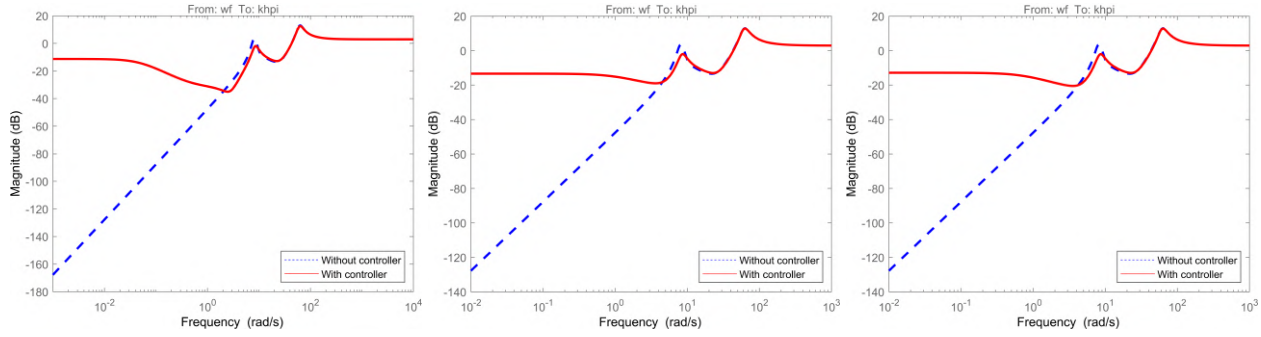

(a) (b) (c)

Figure 5: Frequency response of the relative displacement: a) design 1; b) design 2; c) design 3

5.3 Analysis of vertical acceleration in time

Another performed analysis observed the behavior of the responses in time, Fig. 6 presents the response in time of the vertical acceleration. Under this aspect, the system without control had a settling time of 3.6 seconds and a peak response of 8.76 m/s^2. While for design 1 there was a 68.0 $\%$ reduction in the settling time and a 95$\%$ reduction in the peak response. For design 2, the reduction in settling time was 70.0 $\%$ and a 46.3 $\%$ reduction in peak response. Finally, for design 3, the reduction in settling time was 66.8 $\%$ and a 50.7 $\%$ reduction in peak response. Additionally, Tables 6 and 7 present the settling time and peak values for the vertical acceleration, both considering the nominal condition and the extreme conditions, considering the uncertainties.

5.4 Analysis of relative displacement in time

The next time analysis was given comparing the responses of the contact index with the track, in Fig. 7 is presented the response in time of the contact index between the tire and the track. Under this consideration, the results showed that the uncontrolled system had an accommodation time of 0.4 seconds and a peak response of 0.20 m/s^2. While, for the

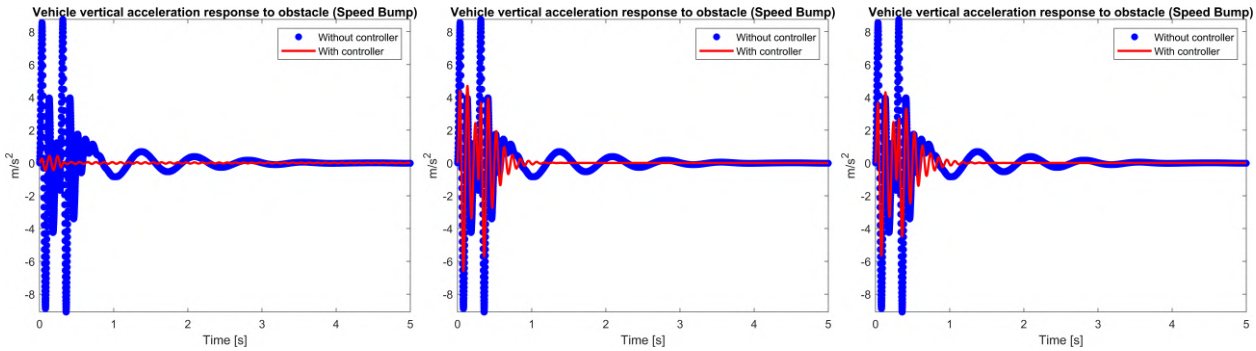

(a) (b) (c)

Figure 6: Vertical acceleration in time: a) project 1; b) project 2; c) project 3

Table 6: Table of vehicle vertical acceleration settling times ($t_{s_{z_1}}$) resulted from the simulation with obstacle

Cases	$t_{s_{z_1}}$ Passive [s]	$t_{s_{z_1}}$ P1 [s]	Δ%P1	$t_{s_{z_1}}$ P2 [s]	Δ%P2	$t_{s_{z_1}}$ P3 [s]	Δ%P3
1	3.387	7.032	-107.6	1.028	69.6	1.136	66.5
2	2.707	9.458	-249.5	1.189	56.1	1.393	48.5
3	4.139	7.128	-72.2	1.159	72.0	1.268	69.4
4	4.087	9.554	-133.8	1.326	67.5	1.485	63.7
5	3.804	6.112	-60.7	0.959	74.8	1.081	71.6
6	2.780	8.212	-195.5	1.151	58.6	1.326	52.3
7	4.252	6.049	-42.3	1.008	76.3	1.127	73.5
8	4.571	8.149	-78.3	1.188	74.0	1.370	70.0
Nominal	3.595	1.150	68.0	1.078	70.0	1.192	66.8

Table 7: Table of vehicle vertical acceleration peaks resulting from obstacle simulation

Cases	max(z_1) Passive [m/s^2]	max(z_1)P1 [m/s^2]	Δ%P1	max(z_1)P2 [m/s^2]	Δ%P2	max(z_1)P3 [m/s^2]	Δ%P3
1	9.994	0.557	94.4	7.252	27.4	6,139	38.6
2	13.297	0.568	95.7	8.249	38.0	6.920	48.0
3	9.442	0.570	94.0	7.533	20.2	6.494	31.2
4	12.475	0.578	95.4	8.290	33.5	6.919	44.5
5	7.179	0.403	94.4	5.431	24.3	4.719	34.3
6	9.584	0.409	95.7	6.291	34.4	5.292	44.8
7	6.546	0.394	94.0	5.333	18.5	4.656	28.9
8	8.831	0.401	95.5	6.102	30.9	5.162	41.5
Nominal	8.755	0.437	95.0	4.700	46.3	4.311	50.7

conditions with the use of the controllers, the settling time did not change for projects 2 and 3, while for project 1 there was an increase of 0.2 m/s^2. The response peak presented an increase of 1.0, 0.7, and 0.9, respectively for projects 1, 2, and 3. Additionally, Tables 8 and 9 detail the information of the accommodation time and peak values for the relative displacement index, both considering the nominal condition and the extreme conditions, considering the uncertainties.

5.5 Actuators Power Analysis

Last but not least, this paper also brings an analysis of the power of the actuators. Here we observe that design 1 presented very high levels of power of the actuators of the active suspension, considering a desirable limitation of 20 kW, as a restriction of commercial specification given by dos Santos (2010). Thus, to meet this restriction, we have designs 2 and 3. In such a way that project 2 presents the lowest levels of maximum power, while project 3 is with power levels closer to the specified limit.

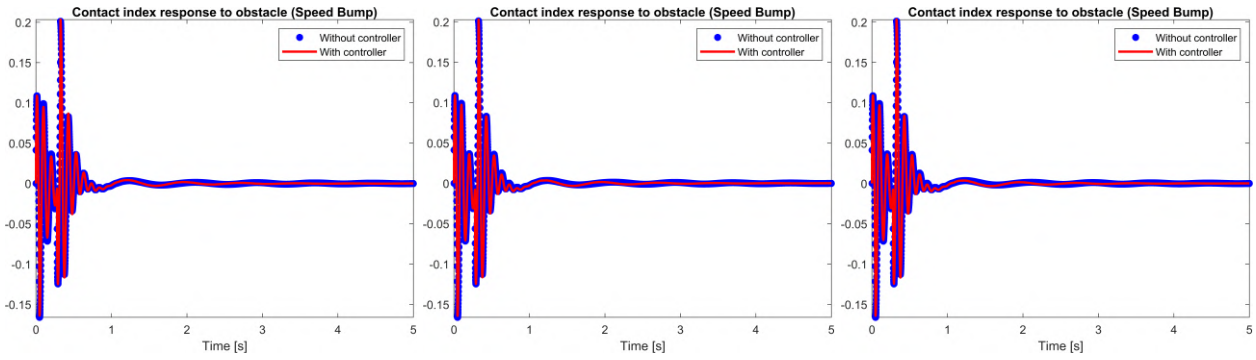

(a) (b) (c)

Figure 7: Relative displacement in time: a) project 1; b) project 2; c) project 3

Table 8: Table of accommodation times of the track contact index ($t_{s_{z_3}}$) resulting from the simulation with obstacle

Cases	$t_{s_{z_3}}$ Passive [s]	$t_{s_{z_3}}$ P1 [s]	Δ%P1	$t_{s_{z_3}}$ P2 [s]	Δ%P2	$t_{s_{z_3}}$ P3 [s]	Δ%P3
1	0.435	0.437	-0.5	0.435	0	0.435	0
2	0.435	0.437	-0.5	0.435	0	0.436	-0.2
3	0.437	0.521	-19.2	0.472	-8	0.472	-8
4	0.437	0.521	-19.2	0.472	-8	0.472	-8
5	0.451	0.452	-0.2	0.450	0.2	0.451	0
6	0.451	0.452	-0.2	0.451	0	0.452	-0.2
7	0.456	0.456	0	0.456	0	0.456	0
8	0.456	0.456	0	0.456	0	0.456	0
Nominal	0.444	0.445	-0.2	0.444	0	0.444	0

Table 9: Table of peak track contact index results from simulation with obstacle

Cases	max(z_3) Passive	max(z_3)P1	Δ%P1	max(z_3)P2	Δ%P2	max(z_3)P3	Δ%P3
1	0.197	0.201	-1.9	0.198	-0.6	0.198	-0.6
2	0.197	0.201	-2.1	0.198	-0.8	0.198	-0.8
3	0.198	0.202	-2.3	0.199	-0.8	0.199	-0.8
4	0.197	0.202	-2.5	0.199	-1.0	0.199	-1.0
5	0.185	0.186	-0.7	0.186	-0.7	0.186	-0.7
6	0.185	0.186	-0.9	0.187	-1.2	0.187	-1.2
7	0.205	0.205	-0.3	0.206	-0.5	0.206	-0.5
8	0.204	0.205	-0.5	0.206	-0.8	0.206	-0.8
Nominal	0.201	0.203	-1.0	0.203	-0.7	0.203	-0.9

Table 10: Table of peak power resulting from the simulation with obstacle, values above 20 kW were highlighted

	Max. front suspension power [kW]			Max. rear suspension power [kW]		
Cases	**P1**	**P2**	**P3**	**P1**	**P2**	**P3**
1	49.0	14.5	19.7	40.5	13.5	16.6
2	49.9	9.5	11.5	42.0	9.6	11.8
3	39.2	11.4	14.6	30.9	11.0	13.9
4	40.5	8.3	10.0	31.9	6.8	8.8
5	29.5	10.0	11.7	33.8	9.6	12.8
6	30.1	7.0	8.6	34.8	5.5	6.3
7	23.8	8.5	10.0	27.7	6.6	9.0
8	24.3	9.9	11.9	28.7	7.0	8.5
Nominal	35.5	11.2	14.4	17.1	10.6	14.0

6. CONCLUSIONS

This work proposed the control development of an active suspension system, based on a half-vehicle model, which has 4 degrees of freedom, given by a multivariable model considering four inputs and three outputs. The control method applied was LQR, and it was adopted an optimization approach through the *Pattern Search* approach, to determine the weights of the matrices used in the controller design.

Finally, as result, it can be concluded that it was possible to obtain a reduction of settling times of vertical accelerations and the peaks of vertical accelerations, on top of the characteristics of relative displacements being little affected, resulting in a suspension system that provides greater comfort for passengers and drivers and still maintains the safety characteristics and controllability of the vehicle. Additionally, to perform the control, the actuators presented a power lower than 20 kW, a restriction imposed from a commercial actuator example.

For future work recommendations, there are other types of inputs to perform the simulation, such as applying track profiles according to the ISO standard, in addition to considering an analysis of the variation of the vehicle speed. Further, it is possible to employ an observer project with the controller project, such as applying a Kalman Filter. Another pertinent suggestion is to apply the control to other models, such as the 2 and 7 DOF. Additionally, the last suggestion is the use and comparison of other optimization algorithms.

7. Acknowledgments

The authors thank the help from Professor Adriano Almeida Gonçalves Siqueira from the University of São Paulo São Carlos School of Engineering. As well as to the Coordenação de Aperfeiçoamento de Pessoal de Nível Superior (CAPES) and Conselho Nacional de Desenvolvimento Científico e Tecnológico (CNPq) for the scholarship provided. Maíra M. da Silva is thankful for her scholarship CNPq 301338/2018-3. Felipe M. Farias Filho is thankful for his scholarship CAPES 88887.511682/2020-00.

8. REFERENCES

Darus, R. and Sam, Y.M., 2009. "Modeling and control active suspension system for a full car model". In *2009 5th International Colloquium on Signal Processing Its Applications*. pp. 13–18. doi:10.1109/CSPA.2009.5069178.

dos Santos, M.M., 2010. *Controle H-infinito em suspensões ativas aplicando técnicas baseadas em desigualdades matriciais lineares*. mestrado, Universidade Estadual de Campinas, Faculdade de Engenharia Mecânica, Campinas, SP.

Doyle, J.C., 1978. "Guaranteed margins for lqg regulators". *IEEE Transactions on automatic Control*, Vol. 23, No. 4, pp. 756–757.

Gandhi, P., Adarsh, S. and Ramachandran, K., 2017. "Performance analysis of half car suspension model with 4 dof using pid, lqr, fuzzy and anfis controllers". *Procedia Computer Science*, Vol. 115, pp. 2–13. ISSN 1877-0509. doi:https://doi.org/10.1016/j.procs.2017.09.070. 7th International Conference on Advances in Computing & Communications, ICACC-2017, 22-24 August 2017, Cochin, India.

Hasbullah, F. and Faris, W.F., 2010. "A comparative analysis of lqr and fuzzy logic controller for active suspension using half car model". In *2010 11th International Conference on Control Automation Robotics Vision*. pp. 2415–2420. doi:10.1109/ICARCV.2010.5707260.

ISO-2631-1, 2010. "Mechanical vibration and shock: evaluation of human exposure to whole-body vibration. part 1, general requirements–amendment iso 2631-1: 1997/amd 1: 2010".

Kumar, M.S. and Vijayarangan, S., 2006. "Design of lqr controller for active suspension system". *Indian Journal of Engineering and Materials Sciences*, Vol. 13, pp. 173–179.

Nagarkar, M.P. and Patil, G.V., 2012. "Performance analysis of quarter car active suspension system: Lqr and h ∞ control strategies". In *2012 Third International Conference on Computing, Communication and Networking Technologies (ICCCNT 2012)*. IEEE Computer Society, Los Alamitos, CA, USA, pp. 1–6. doi:10.1109/ICCCNT.2012.6396067.

Ogata, K., 2010. *Engenharia de controle moderno*. São Paulo : Pearson Prentice Hall, 5th edition.

Pang, H., Chen, Y., Chen, J. and Liu, X., 2017. "Design of lqg controller for active suspension without considering road input signals". *Shock and Vibration*, Vol. 2017. doi:10.1155/2017/6573567.

Rao, S.S., 2019. *Engineering optimization: theory and practice*. John Wiley & Sons.

SUN, W., GAO, H. and SHI, P., 2020. *Advanced control for vehicle active suspension systems*. Springer International Publishing.

9. RESPONSIBILITY NOTICE

The authors are solely responsible for the printed material included in this paper.